Blood-Sucking Leech Optimizer for Energy Loss Reduction in Distribution Power Networks with the Integration of Distributed Solar Generators

Xuan Hoa Thi Pham[1], Quynh Vu Nguyen[2], Minh Van Nguyen[3], and Bach Hoang Dinh[4,*]

ARTICLE INFO

Article history:
Received: 14 June 2025
Revised: 13 November 2025
Accepted: 25 December 2025
Online: 20 July 2026

Keywords:
Entire electricity power loss
Distribution electricity power grid
Distributed solar generators
Sand cat swarm optimization
Blood-Sucking Leech Optimizer

ABSTRACT

This research investigates the application of two recently proposed meta-heuristic algorithms, the Sand Cat Swarm Optimization (SCSO) and the Blood-Sucking Leech Optimizer (BSLO), for optimizing the allocation of Distributed Solar Generators (DSGs) within the IEEE 85-node distribution electric power grid (DEPG). The primary objective is to minimize entire energy loss (EEL). Firstly, SCSO and BLSO are applied to determine the best allocation solution to DSGs on the large-scale DEPG with 85 nodes in the designing phase under two cases with different configurations of DSGs, including Case 1, where DSGs are configured to inject only active power to the grid, and Case 2, where all the DSGs can inject both active and reactive power to the grid. The results from these initial two cases demonstrated that the BSLO algorithm significantly outperformed SCSO in terms of convergence speed and stability. Particularly, BLSO reaches the similar best EEL as SCSO in Case 1, but BLSO outperforms SCSO in the other criteria in this case, such as the average EEL, maximum EEL, and the standard deviation (STD). In Case 2 with the expanded space solution, BLSO is entirely superior to SCSO in all comparison criteria. Additionally, BLSO has also proven its high performance compared to the other algorithms in both cases. Based on the proven effectiveness, BSLO was then reapplied to address the problem, considering operational aspects, which include variations in load demand and dynamic power supplied by DSGs. The operational simulation is conducted by using load demand variations for the first month of each of the four quarters of a year, along with actual power data supplied by DSGs. The findings indicate that the integration of DSGs yielded improvements of EEL up to 24.55% in January, 25.68% in April, 24.70% in July, and 23.81% in October compared to the case without DSGs.

1. INTRODUCTION

Distribution Electric Power Grids (DEPGs) serve as the vital element that connecting in the broader power system, acting as the final stage of electricity delivery. Their primary function is to transform and transport high-voltage power received from the main transmission network, which carries electricity over long distances, and then distribute it to meet the diverse and localized demands of consumers, industries, and commercial establishments. Given their intermediate position, acting as the bridge between the high-voltage transmission backbone and the end-users, the robustness and stability of DEPGs are paramount. The use of consuming devices, like electric vehicle charge stations, can support the integration of renewable power sources into power systems [1]. Any instability or inefficiency within these grids can have widespread consequences, directly impacting the operational characteristics and reliability of all interconnected devices, from household appliances to sensitive industrial machinery [2]. For instance, voltage fluctuations, power outages, or poor power quality within a DEPG can lead to equipment damage, production losses, and significant inconvenience for consumers. Therefore, maintaining a healthy and stable DEPG is crucial to maintain ovarall quality power supply.

Moreover, a characteristic feature of DEPGs, particularly when compared to traditional transmission power systems, is their generally greater physical length and intricate branching structure. Transmission lines typically cover vast distances with fewer connection points and are designed for bulk power transfer. In contrast, DEPGs are designed to

[1]*Department of Electrical and Electronic Engineering, Ho Chi Minh City University of Industry and Trade, Vietnam. Email: hoaptx@huit.edu.vn.*
[2]*Faculty of Electrical and Electronics, Lac Hong University, Dong Nai 810000, Vietnam. Email: vuquynh@lhu.edu.vn.*
[3]*Faculty of Electrical and Electronics Engineering, Ho Chi Minh City University of Technology and Engineering, Ho Chi Minh City, Vietnam. Email: minhnv.ncs@hcmute.edu.vn.*
[4]*Power System Optimization Research Group, Faculty of Electrical and Electronics Engineering, Ton Duc Thang University, Ho Chi Minh City, Vietnam.*
**Corresponding author:* Bach Hoang Dinh; Phone: +84-983-842-656; Email: dinhhoangbach@tdtu.edu.vn.

supply energy to neighborhoods, streets, and buildings, leading to a much more extensive and complex network of feeders and laterals. This extended length and increased complexity contribute to a higher overall active power loss during electricity transmission within the various branches of the distribution network [3]. These losses, mainly due to the resistance of conductors, lead to heat and represent wasted energy. For these reasons, minimizing the entire active power loss (EAPL) is not merely an operational goal but a fundamental priority that permeates every stage of a specific DEPG's lifecycle – from its initial conceptual design and meticulous planning to its physical construction and ongoing daily operation [4]. Reducing EAPL can improve energy efficiency, shorten the overall operating costs for utilities, and reduce emissions because less power needs to be generated to meet the same demand. Therefore, for EAPL, reduction is a clear criterion to indicate the overall efficiency and sustainability of the whole distribution system [5]. The integration of sustainable energy sources like solar and wind power has gained significant traction recently. This shift is driven by the urgent need to alleviate pressure on our existing power systems, which are struggling to meet the growing and unpredictable growth of electricity demand [6], especially when electric vehicle charging stations (EVCS) have recently been considered to be placed on DEPGs [7]. Furthermore, placing distributed generators (DGs), especially those based on renewable energy, offers a cost-effective and environmentally friendly way to combat global warming [8] and voltage improvement [9].

Beyond their environmental benefits of reducing the EAPL value, the proper placements of distributed solar generators (DSGs) and distributed wind generators (DWGs) offer noticeable operational advantages. Particularly, these DSGs can help reduce power loss in distribution lines by lowering current amplitude and improving voltage stability across the grid, leading to a better overall voltage deviation index [10]. However, these benefits are only fully realized when the placement of DSGs is optimized on the considered grid [11]. In [12], the authors indicate that the optimization of DGs on any DEPGs is dependent on two key parameters: the rated powers of the DGs and their positions on the grid. One approach to solving this optimization problem, as explored in [12], involves using a meta-heuristic algorithm called Sea Horse Optimization (SHO). In this method, SHO is in charge of producing a set of potential solutions for both the rated power and location within a defined range. These parameters then serve as inputs for a power flow calculation tool, such as the backward and forward sweep (BFWs) method. The BFWs tool calculates the objective function values, which are the targets researchers aim to optimize (e.g., minimizing power loss or improving voltage). The combination of rated power and position that yields the best objective function value is then identified as the optimal solution.

Having said that, the role of meta-heuristic based-computing methods is highly important to the final results. Such algorithms can provide a large set of potential solutions as one using the computing capability of a modern central processing unit (CPU) instead of one by one as other old-fashioned computing methods, which are based on deterministic approaches. The promising capabilities demonstrated in many studies unfold the problem of optimizing the allocation of renewable energy in the grid. Particularly, the Population-Based genetc algorithm (PGA) is applied in [13] to determine the optimal placement of the wind-based distributed generators to two DEPGs, the IEEE 33 and 69-node for three different objective functions, including 1) minimizing operating cost, 2) minimizing power losses, and 3) minimizing the total emission. Note that, the PGA used in [13] is not a improved or modified version from Genetic algorithm (GA), the algorithm is proposed based on the simulation of evoluationary process of human, and other living entities using the rule of improving in decendent generation. Next, the authors in [14] applied a cutting-edge meta-heuristic algorithm called the Osprey Optimization Algorithm (OOA) to optimize the designed parameters of distributed generators in terms of their size and site on the IEEE 33, 118-node, and a practical DEPGs with 54 nodes in Malaysia for power loss reduction. Additionally, various types of DGs have been considered for integration into the given DEPGs to quantify the effectiveness of each placement solution in terms of the power loss index and to evaluate the actual performance of OOA compared to others. Next, the Jellyfish Swarm Algorithm (JSA) is applied to optimize the placement of DSGs in the IEEE 33-node system in different scenarios with varying DSG quantities [15]. A comprehensive evaluation of JSA is provided based on its effectiveness in addressing a multi-objective function, which encompasses the reduction of power loss, minimization of the voltage deviation index, and enhancement of the voltage stability index. The results have clearly indicated that JSA provides the best search performance in handling the nonlinear and highly complex constraints featured by the given optimization problem. Moreover, the implementation of other meta-heuristic algorithms to solve the mentioned problems, including Red Fox Optimisation (RFO) [16], Particle swarm optimization (PSO) [17], Mixing and Exploring Algorithm (MEXA) [18], Improved Fire Hawk Optimizer (IFHO) [19], Subtraction-Average Algorithm (SAA) [20], Artificial Ecosystem Optimizer (AEO) [21], Jellyfish search algorithm (JSA) [22], the modified whale optimization algorithm (MWOA) [23], Artificial ecosystem-based optimizer opposition-based learning (AEO-OBL) [24], Revised coyote optimization algorithm (RCOA) [25], Improved Equilibrium optimizer (IEO) [26], Chimp Sine Cosine Algorithm (ChSCA) [27], Red Fox Path Finder Algorithm (RPFO) [28], Puma optimizer (PO)

[29], Improved Frilled Lizard algorithm (IFLA) [30], and Rat Swarm Optimization (RSA)[31].

Acknowledging the robust capabilities of meta-heuristic based-computing methods in optimizing the allocation of Green Energy Sources (GESs) in Distributed Electric Power Generation (DEPG) systems, this study employs two recently proposed meta-heuristic algorithms: the Sand Cat Swarm Algorithm (SCSA) [32] and the Blood-Sucking Leech Optimizer (BSLO) [33]. Our objective is to optimize the allocation of Distributed Solar Generators (DSGs) within a large-scale IEEE 85-node DEPG system, primarily aiming to minimize the entire active power loss (EAPL). The SCSA algorithm is inspired by the hunting behaviors of sand cats, specifically their searching and attacking phases. Its developers claim that SCSA offers an excellent balance between exploration and exploitation during the search process, demonstrated through its application to various test suites, including CEC-2019 and other optimal design problems, outperforming previous algorithms. Conversely, BSLO models the foraging behavior of blood-sucking leeches in rice fields. Similar to SCSA, BSLO has been validated against CEC-2017 and 2019 benchmarks, as well as practical optimization problems, proving its advantages over many existing algorithms. In summary, the selection of SCSO and BLSO to employ in this study is based on the following advantages compared to previous studies:

- Both SCSO and BLSO provide high performance in dealing with various optimization problems compared to others, as mentioned.
- The update method for new solutions of SCSO and BLSO is based on the strong foundation derived from nature, with assessed efficiency. Particularly, SCSO simulates the searching and hunting behavior that plays a vital role in surviving and developing the whole swarm in harsh conditions. BLSO, on the other hand, mimics the foraging practice of the blood-scucking leeches, which help this species survive through many generations
- The update method for new solutions of SCSO and BLSO is based on the strong foundation derived from nature, with assessed efficiency. Particularly, SCSO simulates the searching and hunting behavior that plays a vital role in surviving and developing the whole swarm in harsh conditions. BLSO, on the other hand, mimics the foraging practice of the blood-scucking leeches, which help this species survive through many generations, regardless of the inconvenience from the weather.

The novelties of the study are listed as follows:

- This research introduces the application of two recently proposed metaheuristic techniques - Sand Cat Swarm Optimization (SCSO) and Blood-Sucking Leech Optimizer (BSLO) - to solve the optimal allocation problem of Distributed Solar Generators (DSGs) in a large-scale DEPG consisting of 85 buses.
- The study explicitly models the 24-hour temporal variation of the entire active power loss (EAPL) in the investigated DEPG, followed by a comprehensive estimation of cumulative energy losses on both monthly and annual bases.
- Realistic solar generation profiles are incorporated by utilizing actual solar irradiance data sourced from the Global Solar Atlas, enhancing the accuracy and practical relevance of the proposed framework.

The striking contribution of the whole study are summarized as follows:

- Extensive case studies are conducted to assess the impact of various DSG allocation strategies on the defined objective functions, with detailed numerical results reported and discussed.
- Through systematic comparative analyses, the BSLO algorithm is identified as the most effective approach among the investigated methods, consistently outperforming SCSO across multiple operating scenarios.
- The performance of the BSLO is further benchmarked against previously reported optimization techniques in the literature, clearly demonstrating its superior robustness and solution quality for the addressed problem.
- An in-depth investigation is carried out to quantify the influence of DSG penetration in DEPG systems on the EAPL under two distinct operating conditions, providing valuable insights into loss-reduction mechanisms.

The rest of this study is organized as follows: Section 2 details the mathematical model of the optimization problem, including the main objective function and relevant constraints. Section 3 provides a brief introduction to the algorithms applied in this research. Section 4 presents the case studies and the results achieved by the two algorithms. Lastly, Section 5 highlights the key findings and contributions of the entire study.

2. PROBLEM MODELLING

2.1. The objective function.

As previously stated, this study aims to minimize the entire active power loss (EAPL) resulting from power transmission across all branches of the investigated distribution electric power grid. The mathematical expression for this primary objective function is as follows [14]:

$$Minimize\ EAPL = \sum_{br=1}^{N_{Brs}} R_{br} \times I_b^2 \tag{1}$$

where, $EAPL$ in kW is the entire active power loss; N_{Brs} is the of existing distribution lines (branches) in the considered DEPG; R_{br} is the branch's resistance *br*; and I_{br} is the current amplitude circulate of branch *br*.

2.2. The involved constraint

2.1.1. The constraint of power balance

This constraint is applied for both active and reactive power in the DEPG, meaning that the entire power generated by all the existing sources must equal the amount of power demanded by load plus the amount of power loss [13]:

$$AP_S + \sum_{s=1}^{N_{DSG}} AP_{SG,s} = AP_{DM} + AP_L \quad (2)$$

and

$$RP_S + \sum_{s=1}^{N_{DSG}} RP_{SG,s} = RP_{DM} + RP_L \quad (3)$$

In Equations (2) and (3), AP_S and RP_S are the active and reactive power at the slack bus which is normally known as the first node of the considered DEPG; $\sum_{s=1}^{N_{DSG}} AP_{SG,s}$ and $\sum_{s=1}^{N_{DSG}} RP_{SG,s}$ are the total active and reactive generated by all the DSGs connected to the considered DEPG; $AP_{SG,s}$ and $RP_{SG,s}$ are the active and reactive power supplied by the DSG *s*; AP_{DM} and RP_{DM} are the active and reactive power required by consuming end; AP_L and RP_L are the active and reactive power loss.

2.1.2. The working constraint of the DSG

This constraint is imposed to ensure that the DSGs connected to the grid will be operated within their design limitation for safety and stability [14]:

$$AP_{SG,s}^{min} \le AP_{SG,s} \le AP_{SG,s}^{max} \quad (4)$$

$$RP_{SG,s}^{min} \le RP_{SG,s} \le RP_{SG,s}^{max} \quad (5)$$

where, $AP_{SG,s}^{min}$ and $AP_{SG,s}^{max}$ are the minimum and maximum active power supplied by the DSG *s*; $RP_{SG,s}^{min}$ and $RP_{SG,s}^{max}$ are the minimum and maximum amount of reactive power injected to grid by the DSG *s*;

2.1.3. The constraints of power factors

In this research, the DSG is supposed to be operated with a power factor varied between 0.85 and 1.0 as follows [21]:

$$Pf_{SG,s}^{Min} \le Pf_{SG,s} \le Pf_{SG,s}^{Max} \quad (6)$$

where, $Pf_{SG,s}^{Min}$ and $Pf_{SG,s}^{Max}$ are the lowest and highest indexes of the power factor of the DSG *s*; $Pf_{SG,s}$ is power factor value of the DSG *s*.

2.1.4. Constraint of position for placing DSG

According to [4], the legal position to place a DSG in the considered DEPG is stated as follows:

$$2 \le L_{DSG,s} \le N_{No} \quad (7)$$

where, $L_{DSG,s}$ is the legal position of the DSG s on the given DEPG.

2.1.5. The constriant of voltage and current values

Voltage node and current branch are the two operational parameters that directly affect the effectiveness and stability in the operation of all the devices connected to the considered DEPG; therefore, this parameter must be manipulated in the safety ranges as stated below [4]:

$$V_{No}^{Min} \le V_{No} \le V_{No}^{Max} \quad (8)$$

$$I_{br} \le I_{br}^{max} \quad (9)$$

where, V_{No}^{Min} and V_{No}^{Max} are the lowest and highest indexes of voltage magnitude at nodes, which are specified as 0.95 and 1.05 p.u; V_{No} is the voltage magnitude of the node *No* in the system; I_{br}^{max} is the largest value electric current flow through branch *br*.

3. THE APPLIED ALGORITHMS

3.1. The Sand cat swarm optimziation

As previously mentioned, the Sand Cat Swarm Optimization (SCSO) algorithm is structured into two main phases: the searching phase and the attacking phase. These phases form the basis of the update mechanism for new solutions during the SCSO's optimization process. The mathematical expression of the two phases are presented below:

- ***The searching phase***

The new location of an individual within the search area in this phase is determined by multiplying the difference between its current position and its best-so-far position by a guiding factor, as follows [32]:

$$C_n^{new,p1} = \left(C_{n-Best,} - \varepsilon \times C_n\right) \times \mu \quad (10)$$

where, $C_n^{new,p1}$ the new location of the individual *n* with *n* = 1, 2, …, *Npo* and *Npo* is the initial population size; $C_{n-Best,}$ is the best location of the individual *n* at the current time; ε is the random value between zero and one; C_n is the current location of the individual *n*; and μ is the guiding factor calculated using the following expression [32]:

$$\mu = scf \times \varepsilon \quad (11)$$

with

$$scf = 2 - \left(\frac{4 \times IT}{IT + IT^{max}}\right) \quad (12)$$

where, scf sensitive coefficient; IT and IT^{max} are the current index of iteraiton and the maximum index of iteration.

- ***The attacking phase***

In this phase, the new location of each individual in the population will be updated for its new location using the following mathematical model [32]:

$$C_n^{new,p2} = C_{GB} - C_{rand} \times cos(\theta) \times \mu \quad (13)$$

where, $C_n^{new,p2}$ is new location of the individual n updated in phase 2; C_{GB} the individual with the best location in the whole population; C_{rand} is the individual random selected from the population; θ the phase angle between the moving directions of the individual *n* to its prey in seach space.

Note the two phases as described above are not executed sequentially but selecting one out of two depending on the comparison of regulating factor (*rgf*) as the following pseudo code:

If *rgf* ≤1

Execute the update process using Equation (10),

Else

Execute the update process using Equation (13) ,

End.

3.2. Blood-Sucking Leech Optimizer.

This section will describe the new solution's update process in the Blood-Sucking Leech Optimizer (BSCO) update process. In general, the update process consists of three phases. The first two phases are similar to SCSO above, which are the exploration and exploitation phases, and expressions will be given as follows:

- ***The exploration phase***

The new position in this phase of each individual in the population is determined based on the disturbance coefficient and the arc length in the four subcases as follows [33]:

$$B_n^{new,p1} = \begin{cases} B_n + DC \times B_n - V_{DC1}, & for\ Case\ 1 \\ B_n + DC \times B_n + V_{DC1}, & for\ Case\ 2 \\ B_k + DC \times B_k - V_{DC2}, & for\ Case\ 3 \\ B_k + DC \times B_k + V_{DC2}, & for\ Case\ 4 \end{cases} \quad (14)$$

with

$$V_{DC1} = rnd_1 \times |GB_n - B_n| \times DT \times \left(1 - \frac{RIG}{Npo}\right) \quad (15)$$

$$V_{DC2} = |GB_n - B_n| \times DT \times \left(1 - rnd_1^2 \frac{RIG}{Npo}\right) \quad (16)$$

Case 1: $rnd\ < 0.97\ and\ |GB_n| > |B_n|$

Case 2: $rnd\ < 0.97\ and\ |GB_n| < |B_n|$

Case 3: $rnd > 0.97\ and\ |GB_n| > |B_n|$

Case 4: $rnd > 0.97\ and\ |GB_n| < |B_n|$

$B_n^{new,p1}$ is the new position *n* updated in the exploaration phase; B_n and B_k the current position n and the neighbor position k which is next potential position; DC is the disturbance coefficient; rnd is the random value between zero and one; GB_n the best position so far of the solution *n*; V_{DC1} and V_{DC2} are the two vector that provide the disturbance; DT is the distance of the leeches from human; RIG is the real integer determined by the change of iteration index compared to one;

- ***The exploitaion phase***

In this exploitation phase, the new positions are updated using the following expression [33]:

$$B_n^{new,p2} = \begin{cases} GB_n + DC \times GB_n - V_{DC3}, & for\ Case\ 1 \\ GB_n + DC \times GB_n + V_{DC3}, & for\ Case\ 2 \\ GB_n + DC \times GB_n - V_{DC4}, & for\ Case\ 3 \\ GB_n + DC \times GB_n + V_{DC4}, & for\ Case\ 4 \end{cases} \quad (17)$$

where

$$V_{DC3} = |GB_n - B_n| \times DT \times \left(1 - rnd_2 \times \frac{RIG}{Npo}\right) \quad (18)$$

$$V_{DC4} = |GB_n - B_k| \times DT \times \left(1 - rnd_2 \times \frac{RIG}{Npo}\right) \quad (19)$$

where, $B_n^{new,p2}$ is the new solution updated in exploitaion phase; V_{DC3} and V_{DC4} are the two vectors that provide disturbance similar to V_{DC1} and V_{DC2}; and rnd_2 is a random value between zero and one.

* *Note that the update mechanism will randomly select one out of two phases described above based on the reference to the term DT compared to 1 using the following pseudo-code:*

If DT ≥1

Execute the update process using Equation (14) ,

Else

Execute the update process using Equation (17),

End.

- ***The stimulating phase***

This phase is only executed when one out of the two phases above is completed. In this phase, the update mechanism is highly dependent on the distance between the best so far solution and the current solution combined with Levy's flight distribution as follows [33]:

$$B_n^{new,p3} = \begin{cases} \dfrac{IT}{IT^{max}} \times |GB_n - B_n| \times LV \times B_n, if\ rnd\ < 0.5 \\ \dfrac{IT}{IT^{max}} \times |GB_n - B_n| \times LV \times GB_n, if\ rnd\ < 0.5 \end{cases} \quad (20)$$

where, $B_n^{new,p3}$ is the new position update in this phase; LV is the value resulted by the Levy's flight distribution.

4. RESULTS AND DISCUSSION

In this section, SCSO and BSLO will be applied to solve the problems mentioned in both planning and operating aspects to minimize the EAPL and the entire energy loss (EEL) in the IEEE 85-node DEPGs. The basic specification of this selected DEPG is cited by [22], and its single-line illustration is depicted in Fig. 1 below. First, the two algorithms will be applied to solve the problem considered in the planning process to evaluate their effectiveness, and then the better-performing algorithm will be reapplied to resolve the problem while considering the operating aspects.

For the planning aspects, the two applied algorithms are in charge of allocating the size and position of DSGs in the given DEPG in two cases below:

- Case 1: Optimizing the placement of 03 DSGs in the given DEPGs that DEPGs only inject active power to grid.
- Case 2: Optimizing the placement of 03 DSGs in the given DEPGs so that DEPGs can inject active and reactive power.

For the operating aspects, the better-performing algorithm between the two will be applied to obtain the EAPL value within 24 hours of an operational day using the actual data of DSG power supply [34], and after that, the EEL value of a month will be determined subsequently. For a fair evaluation, both SCSO and BSLO are preset with the same initial setting parameters in terms of population size (Npo) and maximum iteration (IT^{max}), which are 30 and 200 for Case 1, while these parameters for Case 2 are 50 and 200, respectively. Besides, the SCSO and BLSO were also executed 50 trial tests for their best results in advance of the comparison.

A desktop computer, powered by a 2.5 GHz central processing unit (CPU) and 16 GB of random-access memory (RAM), served as the platform for all computational tasks. All the evolved codings and simulations are executed using MATLAB programming language version 2018a.

4.1. The results achieved in Case 1

Fig. 2 presents the results achieved by SCOS and BSLO throughout their 50-trial test while dealing with the considered problem in Case 1. At first look, both algorithms can achieve the optimal value of EAPL in this case study; however, BLSO offers slight stability compared to SCSO due to its lower fluctuations among the 50-test run.

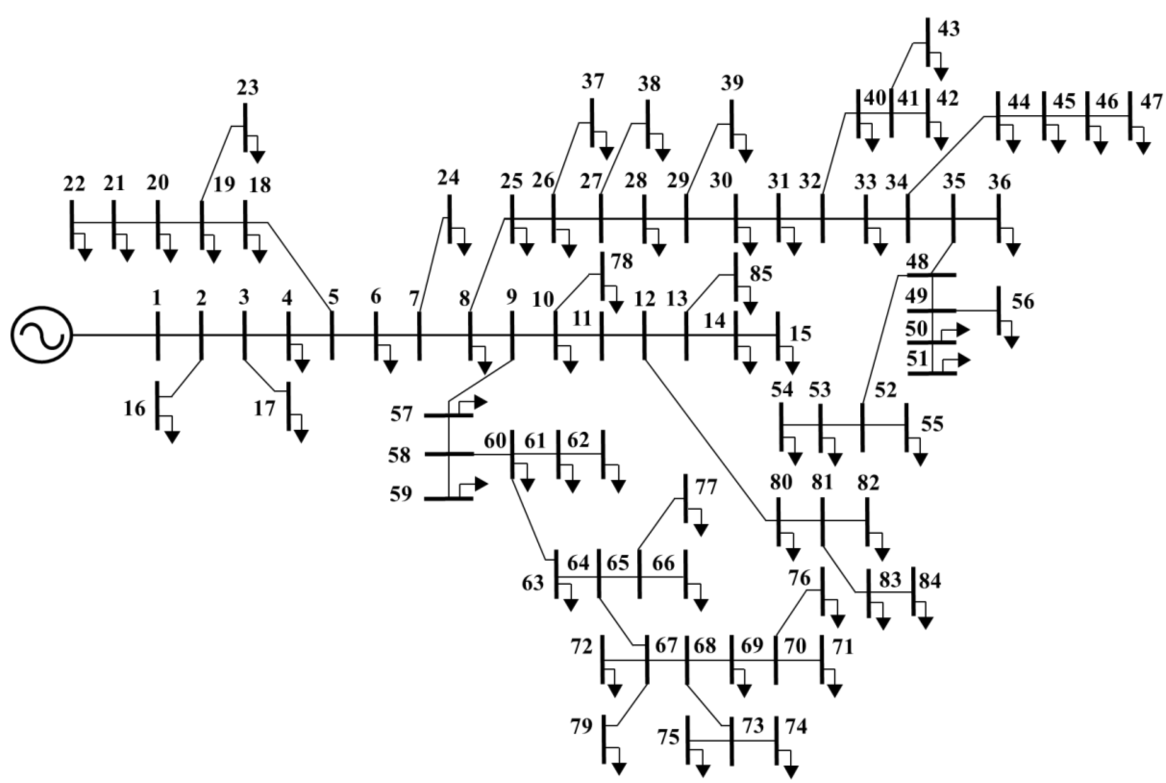

Fig. 1. The description of the IEEE 85-node DEPG.

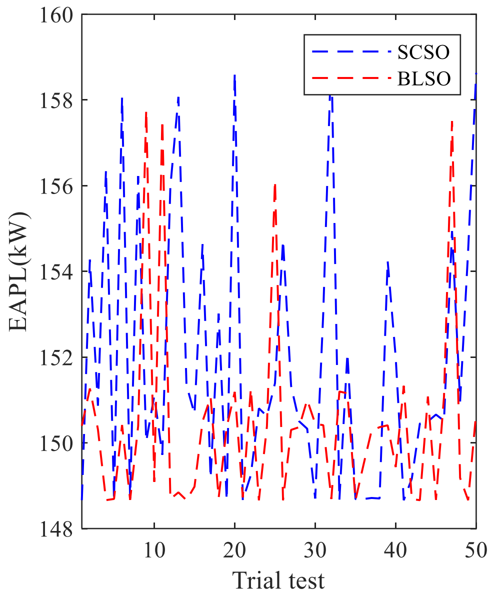

Fig. 2. The results obtained by the two applied algorithms throughout their 50-trial test.

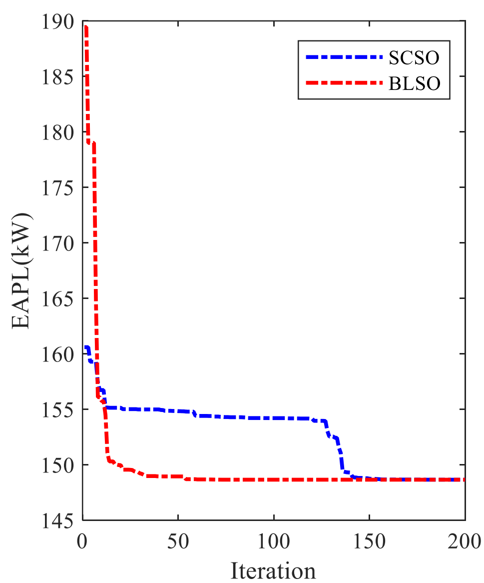

Fig. 3. The minimum convergence characteristics obtained by SCSO and BLSO among 50 trial tests.

Fig. 3, Fig. 4, and Fig. 5, respectively, show the minimum, average, and maximum convergences obtained by the two algorithms. For the minimum convergence presented in Fig. 3, both SCSO and BSLO can achieve the same value of EAPL; however, BLSO shows its faster response in finding the optimized EAPL after 100 iterations only, while SCSO requires over 150 iterations to reach the same result. While Fig. 3 does not clearly demonstrate a superiority of BLSO over SCSO, as these algorithms achieve a similar EAPL at the end of their best runs, Figs. 4 and 5 are presented to provide further evidence of the actual performance of these two algorithms. Particularly, Figs. 4 and 5 provide the average and maximum convergences achieved by SCSO and BLSO across 50 trial tests. The results illustrated in these figures reveal that BSLO is superior to SCSO in these regards.

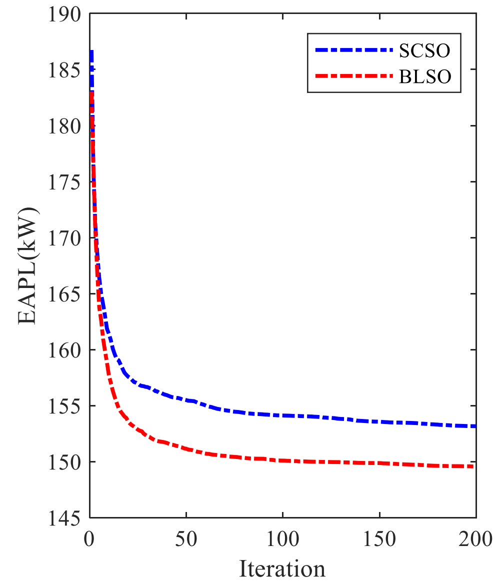

Fig. 4. The average convergence characteristics obtained by SCSO and BLSO among 50 trial tests.

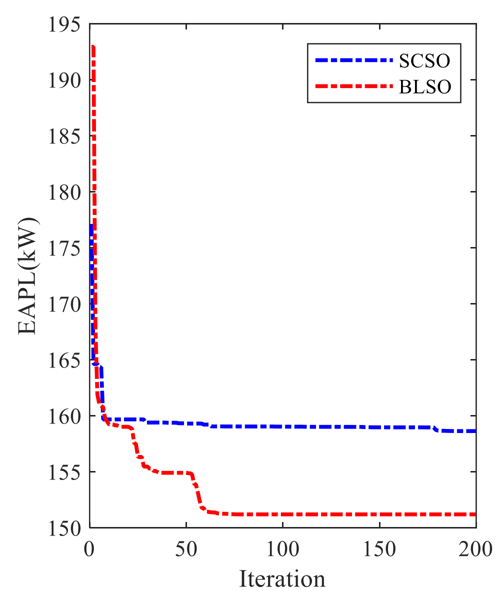

Fig. 5. The maximum convergence characteristics obtained by SCSO and BLSO among 50 trial tests.

Fig. 6 offers a quantitative comparison between the SCSO and BLSO in solving the problem's first case. In particular, three criteria are applied to evaluate the effectiveness of SCSO and BSLO: minimum EAPL, average EAPL, maximum EAPL, and standard deviation (STD). Although SCSO achieved the same value of EAPL as BLSO as presented on the first criteria, the results obtained by

SCSO on the last three criteria are far behind BSLO. Particularly, SCSO achieved 151.845 kW and 159.204 kW for average and maximum EAPL, while the results achieved by BLSO were only 150.437 kW and 157.773 kW for those two criteria. Lastly, the STD of SCSO is up to 3.177, while the similar number of BLSO is only 2.252.

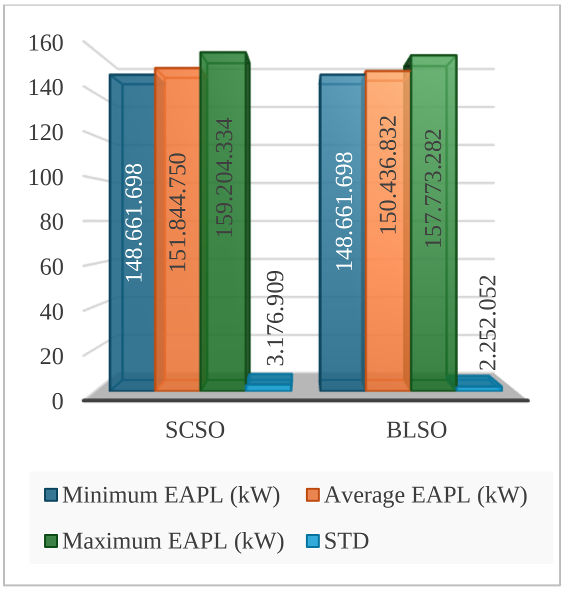

Fig. 6. The results achieved by SCSO and BLSO after their 50-trial test.

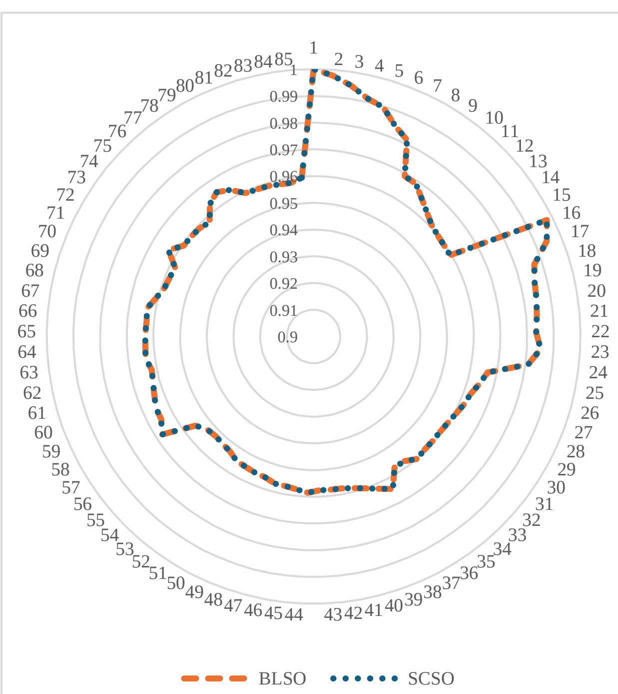

Fig. 7. Voltage nodes resulted by the SCSO and BLSO in Case 1.

Fig. 7 shows the voltage nodes achieved by the BLSO and SCSO in Case 1. It is very clear that there's no difference between the voltage levels achieved by these two algorithms in this case. Also, all the voltage nodes meet the legal boundaries between 0.95 and 1.05 p.u., as explained in Section 2.

Fig. 8 offers a correspondence of the EAPL achieved by SCSO, BLDO, and others previously. Particularly, both SCSO and BLSO are compared to the Sunflower optimization algorithms (SOA), Coyote optimization algorithms (COA), Modified Firefly Algorithm (MFA), and White Shark Optimization Algorithm (WSA).

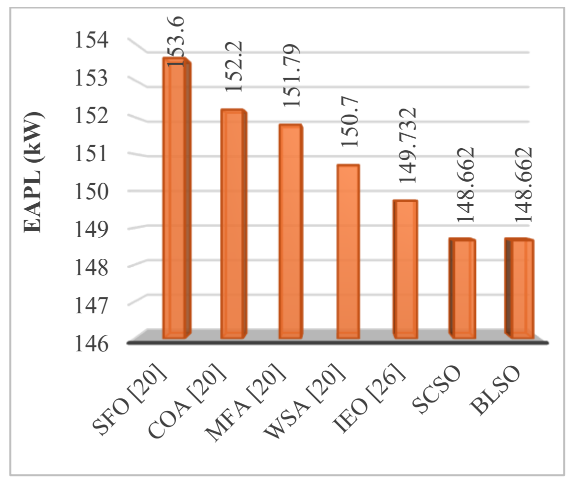

Fig. 8. The comparision between the EAPL achieved by the two algorithms to the previous others.

Table A1 of the Appendix shows the optimial results achieved by SCSO and BLSO in this section.

4.2. The results achiveved in Case 2

In this section, the two algorithms are again applied to optimize the placement of three DSGs in the DEPG considered in Case 1; however, this case supposes that the DSGs can inject active and reactive power to the given DEPG. Mathematically, this case witnessed an increase in the overall complexity of a given problem compared to Case 1. Particularly, SCSO and BLSO in Case 1 must determine two parameters for each DSG placed on the grid, including the location on the grid and the optimal supply power; however, each DSG in Case 2 requires one more parameter, which is the reactive power besides the other two as mentioned earlier.

Fig. 9 presents the EAPL values achieved by SCSO and BLSO throughout their 50 trial tests. In the figure, BLSO is superior to SCSO while dealing with the given problem in Case 2 in terms of the ability to reach the optimal EAPL values and the stability described in the fluctuation degree among all the test runs.

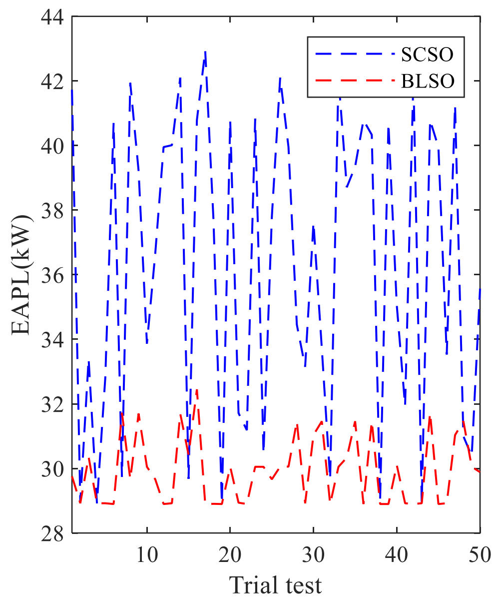

Fig. 9. The resutls obtained by the two applied algorithms throughout 50 trial tests.

Fig. 10, Fig. 11, and Fig. 12, respectively, present the minimum, average, and maximum convergence curves achieved by SCSO and BLSO for their best runs in Case 2. The observation of the three figures indicates that BLSO is entirely superior to SCSO in terms of convergence speed and the optimal value of EAPL.

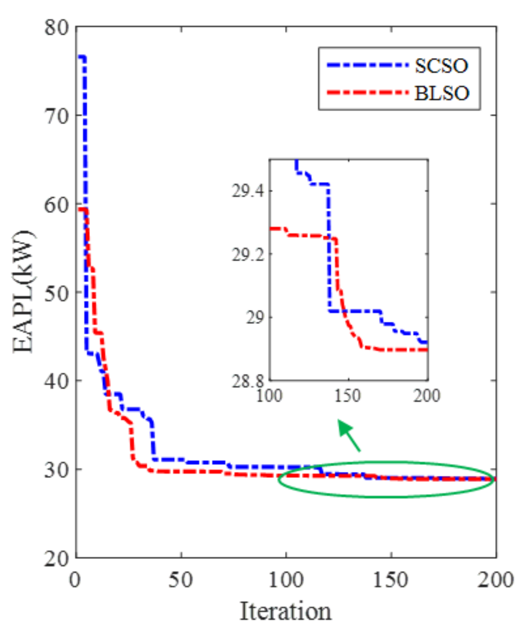

Fig. 10. The minimum convergence characteristics obtained by SCSO and BLSO among the 50 trial tests.

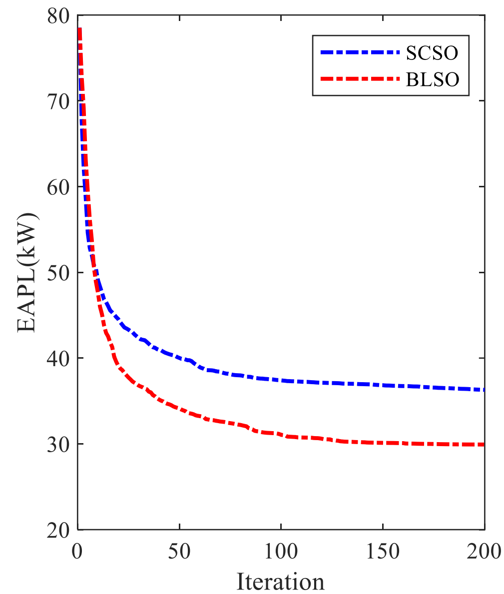

Fig. 11. The average convergence characteristics obtained by SCSO and BLSO among the 50 trial tests.

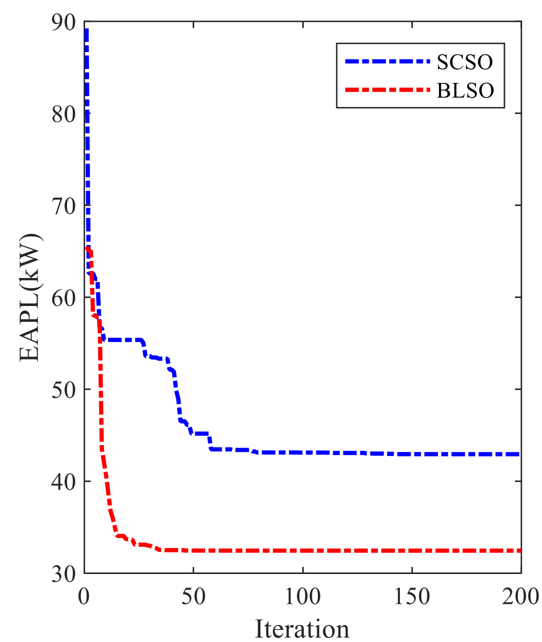

Fig. 12. The maximum convergence characteristics obtained by SCSO and BLSO among 50 trial tests.

Fig. 13 provides a correspondence of the results achieved SCSO and BLSO in Case 2 using different criteria as presented in Fig. 6. Clearly, the expansion of the problem space solution with the additional variable represents the reactive power for each DSGs has clarified the actual performance of the two algorithms. Particularly, the difference in the first criteria between SCSO and BLSO now exists, unlike in Case 1. Regarding the other three criteria, BLSO continues to show an unmatched performance compared to SCSO. For instance, the average and maximum

EAPL obtained by BLSO in Case 2 are 29.920 kW and 32.448 kW, while these similar results achieved by SCSO are 36.297 kW for the Average EAPL and up to 42.937 kW for the Maximum EAPL. Besides, BLSO also proves its surprising stability in Case 2 regardless of the increase in space solution while reaching the STD of only 1.070 compared to SCSO, which has an STD up to 4.791. The differences are huge.

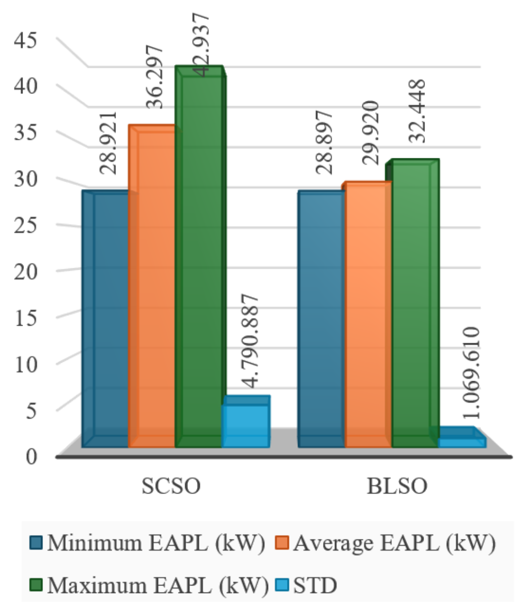

Fig. 13. The results obtained by the two applied algorithms throughout their 50-trial test.

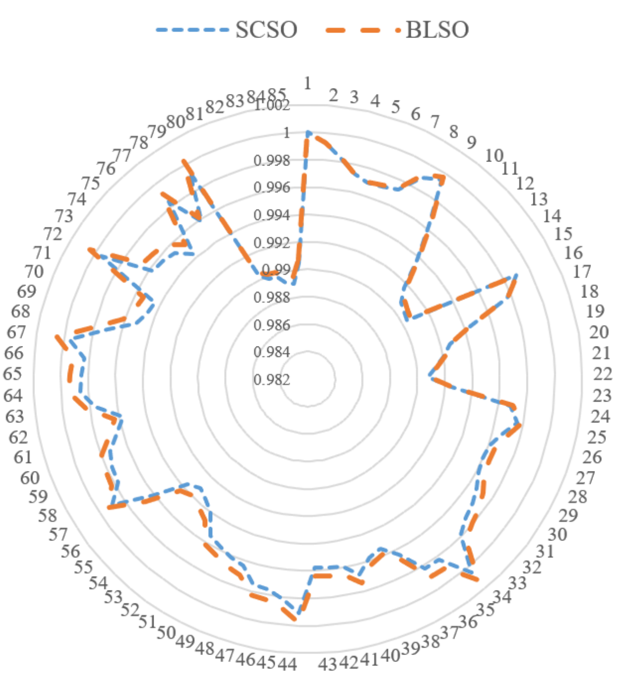

Fig. 14. The voltage nodes achieved by the two algorithms in Case 2.

Fig. 14 shows the voltage nodes achieved by SCSO and BLSO in Case 2. The consideration of the reactive power supply capabilities of DSGs has provided a better improvement in voltage nodes over Case 1. Additionally, the comparison between the two algorithms also indicates that BSLO is the algorithm that offers the better improvement on voltage nodes, which can be observed from node 24 to node 80 of the given DEPG.

Fig. 15 presents the EAPL value achieved by SCSO and BLSO compared to others that previously applied to the problem. After proving the actual effectiveness over SCSO, BLSO also proves itself far more effective than others while solving the considered problem in Case 2. Particularly, BLSO is far more effective compared to FPA [27], CSA [27], AOA [27], and ALO.

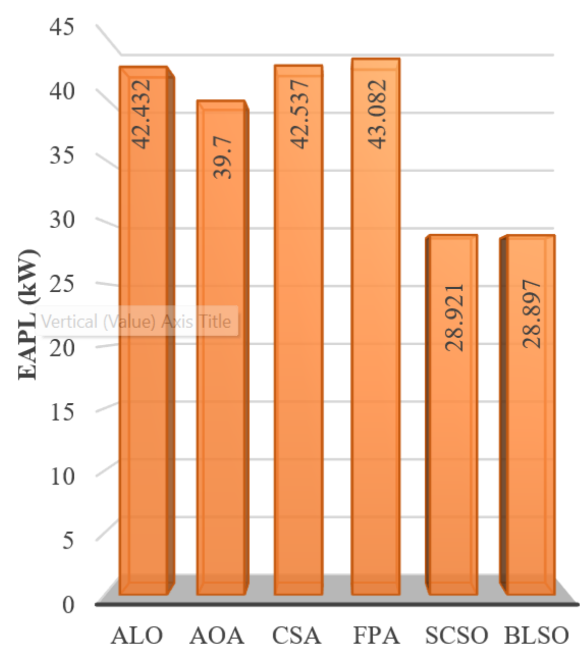

Fig. 15. The comparision of EAPL values between SCSO, BLSO and others.

Table A2 of the Appendix shows the optimial results achieved by SCSO and BLSO in this section.

4.3. The results achiveeved in operation situation

In this section, BLSO is reapplied to solve the problem under operational conditions. This involves accounting for variations in load demand and the dynamic power supply from DSGs, whose capabilities are detailed in Case 1 of Section 4.2. The load demand over 24 hours of an average day in January, April, July, and October is assumed to vary as shown in Fig. 16 [21]. This research supposes that load demand changes according to the four quarters of a year, meaning demand will reshape its profile within 24h every three months. For this reason, these specific months were chosen for the simulations. The power supplied by the three DSGs over 24 hours during these same months is depicted in Figs. 17, 18, and 19. It's important to note that this DSG power supply data is sourced from the Global Solar Atlas [34], an online platform that provides estimated solar power data calculated from radiation measurements worldwide.

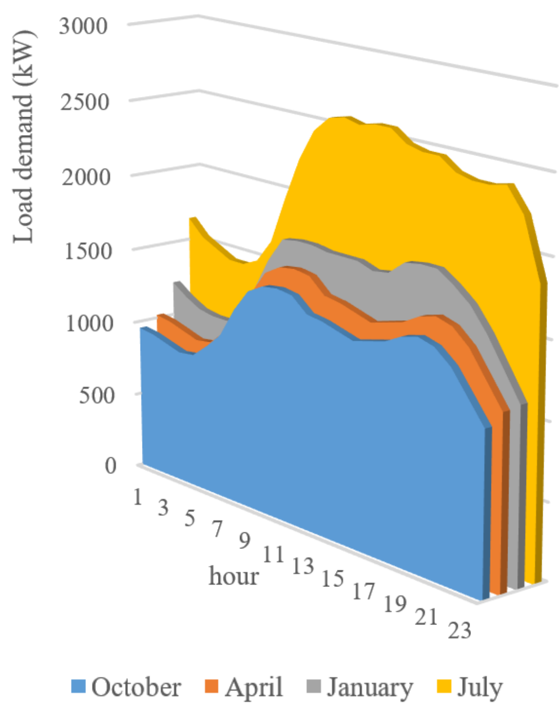

Fig. 16. Load demand variation within 24 hours in an average day of January, April, July, and October.

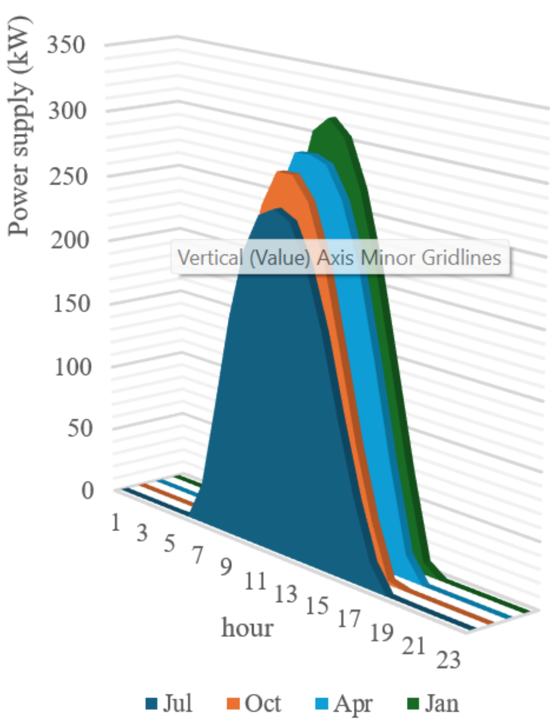

Fig. 17. The active power generated by the DGS1 within 24h of an average day in January, April, July, and October.

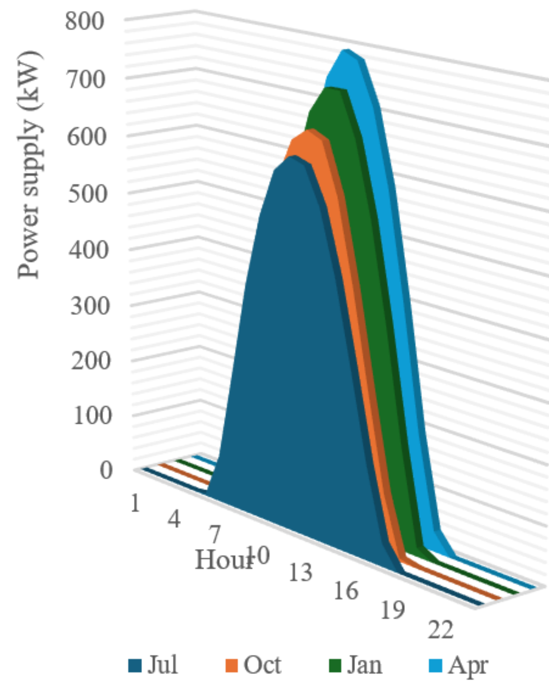

Fig 18. The power supplied by the DGS2 within 24h of an average day in January, April, July, and October.

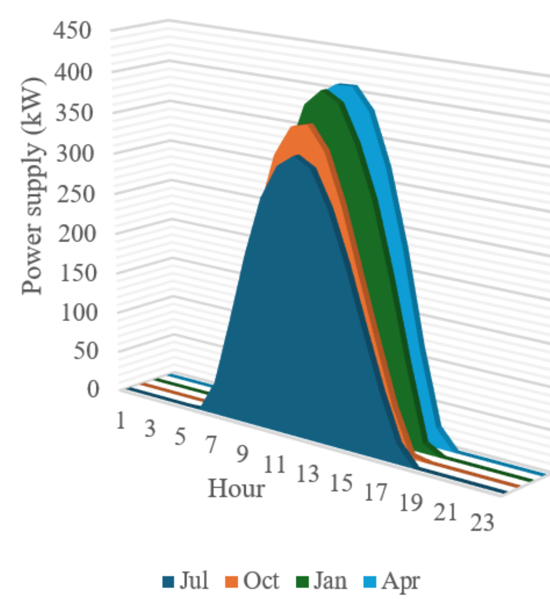

Fig. 19. The active power generated by the DGS3 within 24h of an average day in January, April, July, and October.

Fig. 20 illustrates the hourly EAPL values over a 24-hour period for an average day in January, April, July, and October. The analysis compares two scenarios with and without the integration of DSGs. It is evident that the presence of DSGs leads to a significant reduction in EAPL values during daytime hours, typically from 07:00 to 18:00, corresponding to the operational period of DSGs. The EAPL values remain consistent across both scenarios for the remaining hours of the day. Fig. 21 presents a detailed breakdown of the hourly EAPL reduction. Notably, July exhibits the most substantial reduction in EAPL, whereas October shows the most conservative reduction. It is important to acknowledge that this reduction is exclusively observed during daytime hours, when DSGs are capable of supplying power to the grid only when active, owing to their operational characteristics.

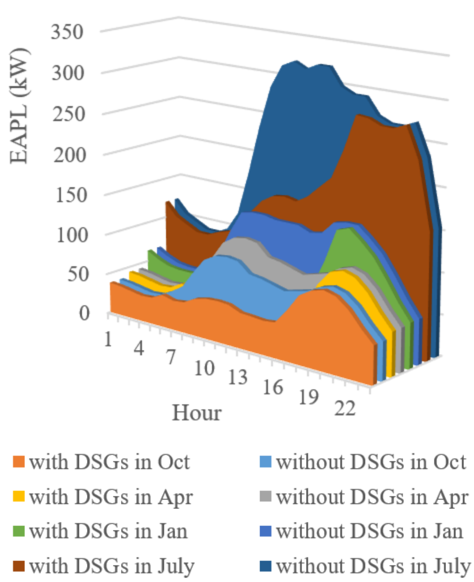

Fig. 20. The EAPL of 24 hours of an average day with/without DSGs of January, April, July, and October.

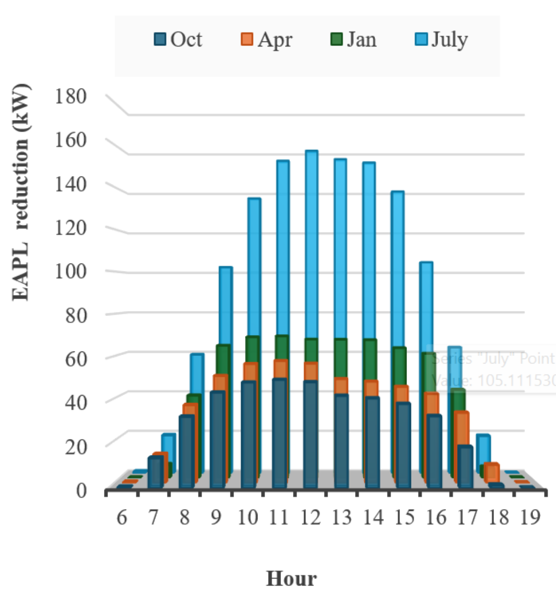

Fig. 21. The EAPL reduction with DSGs of each hour during an average day of January, April, July, and October.

Based on the data of EAPL reduction mentioned in Fig. 21 and Fig. 22, the entire energy loss (EEL) is calculated for each month using Equation (21). The presence of DSG has resulted in a significant improvement in the EEL value. Particularly, the EEL in October has substantially decreased from 50,711.248 kW to 38,260.947 kW, corresponding to a reduction of 24.55%. The April, January, and July reduction percentages are 25.68%, 24.70%, and 23.81%, respectively.

$$EEL_k = n_k \sum_{h=1}^{24} EAPL_h \tag{21}$$

In the Equation (18), EEL_k is the entire energy loss of the month k in a year, n_k is the number of days in a month, n_k can be 30 or 31 in accordance to the considered month.

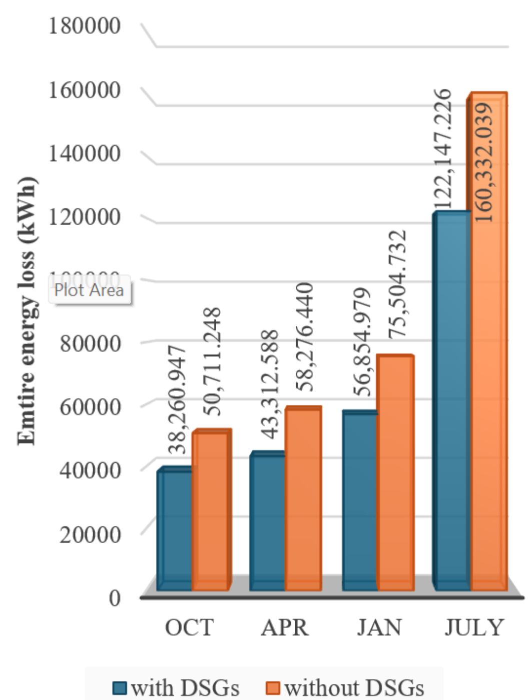

Fig. 22. The EEL value of January, April, July, and October with and without DSG.

Fig. 23, Fig. 24, Fig. 25, and Fig. 26 present the voltage node of the grid corresponding to the four months for the case with DSGs.

5. CONCLUSIONS

In this research, two recently proposed meta-heuristic-based computing methods, including the SCSO and BLSO, are effectively implemented to resolve the problem of optimal allocation of DSGs in the large-scale DEPG for the main objective function of minimizing the EAPL. Besides resolving the given problem in the planning aspect, as in other studies, this study also executes the results achieved in the planning process and applies them to the operation situation with power demand variation and power supply throughout 24h from DSGs. In the planning aspect, BLSO has clearly demonstrated its high effectiveness while dealing with the considered problem compared to SCSO in different comparison criteria in both cases, with different settings of DSGs. Additionally, the effectiveness of BLSO is further enhanced compared to many others. Hence, BLSO is utilized to solve the considered problem in the operating aspect using the results of the sizes and locations of DSGs inherited from the planning aspects. Then the simulation is conducted using the load demand variation and the hourly power injected from DSGs calculated by using real solar data provided by the Global Solar Atlas at certain points in the field. The results reveal that the presence of DSGs in the daytime significantly reduces EAPL within 24 hours and substantially improves EEL value. Particularly, the study chose to simulate the EAPL and EEL in the first month of each quarter in the year, and the results show that the presence of DSGs resulted in the improvement of 24.55%, 25.68%, 24.70%, and 23.81% for January, April, July, and October, respectively. The success of this research is largely attributed to the BLSO, which demonstrated surprising performance and stability throughout different study cases. This capability allowed the algorithm to smoothly handle the given problem, even with increased solution space and heightened complexity when dealing with operational scenarios.

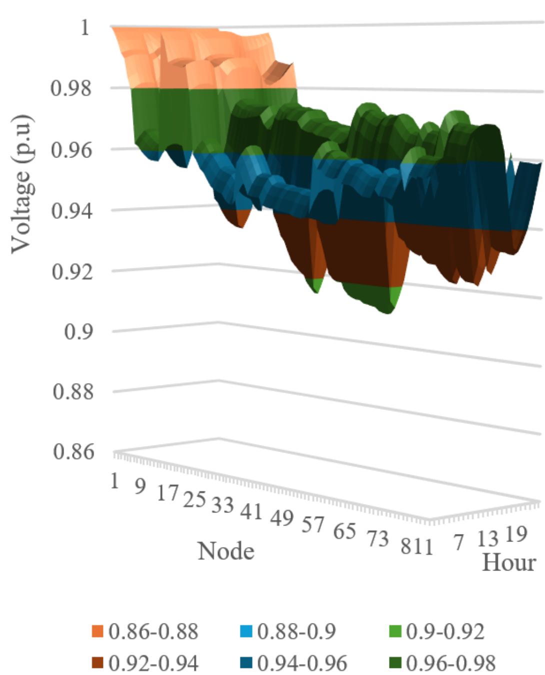

Fig. 23. The voltage node of an average day in January.

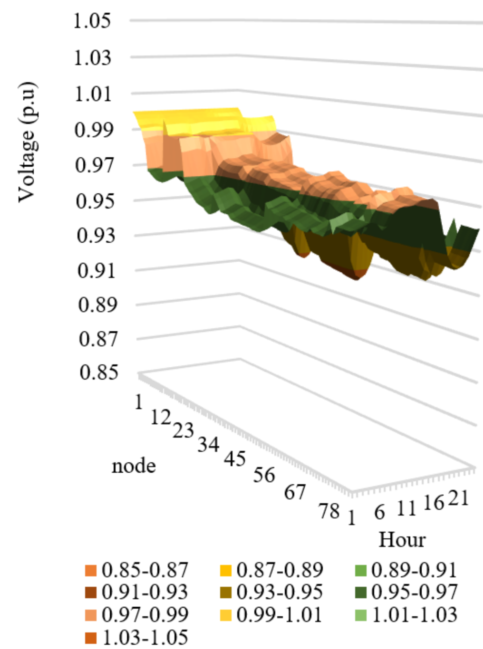

Fig. 24. The voltage node of an average day in April.

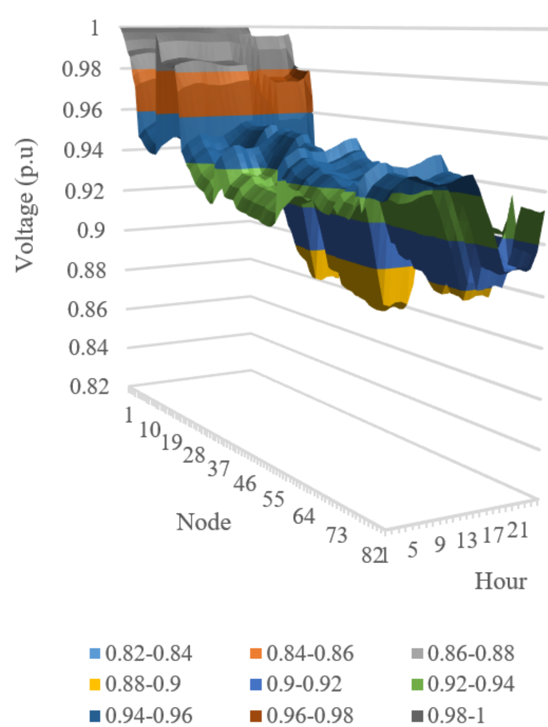

Fig. 25. The voltage node of an average day in July.

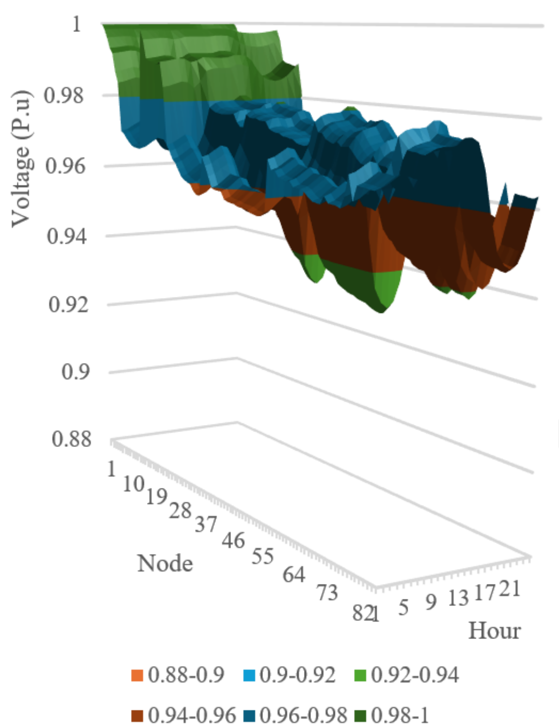

Fig. 26. The voltage node of an average day in October.

REFERENCES

[1] Fokui, W.S.T.; Akupan, R.E.; and Wandji, D.K.N. 2025. Enhancement of the utilization of electric vehicle charging stations in a commercial distribution network. Journal of Advanced Engineering and Computation 9 (4): 184-201. Doi: 10.55579/jaec.202594.512.

[2] Phimtakhob, T., and Chayakulkeeree, K. 2026. Voltage Deviation Improvement in Active Distribution Network Using Battery Energy Storage System Optimal Voltage Droop Control. GMSARN International Journal 20: 237-245.

[3] Moreno Escobar, J.J.; Morales Matamoros, O.; Tejeida Padilla, R.; Lina Reyes, I.; and Quintana Espinosa, H. 2021. A comprehensive review on smart grids: Challenges and opportunities. Sensors 21 (21): 6978. Doi: 10.3390/s21216978.

[4] Duong, M.P.; Le, M.H.; Nguyen, T.T.; Duong, M.Q.; and Doan, A.T. 2025. Economic and Technical Aspects of Power Grids with Electric Vehicle Charge Stations, Sustainable Energies, and Compensators. Sustainability 17 (1): 376. Doi: 10.3390/su17010376.

[5] Van Tran, H.; Phan, T. M.; Truong A. V.; Nguyen, T. T.; and Ton, T. N. 2024. Optimal Allocation of Soft Open Points on Distribution Power Grid with High Penetration of Renewable Energy to Reduce Energy Loss for One day. Proceedings of the International Conference on Green Technology and Sustainable Development. pp. 213-224. Cham: Springer Nature Switzerland. Doi: 10.1007/978-3-031-76232-1_19.

[6] Kong, X.; Feng, L.; Peng, K.; Song, G.; and Xiao, C. 2025. Network and Energy Storage Joint Planning and Reconstruction Strategy for Improving Power Supply and Renewable Energy Acceptance Capacities. Sustainability 17 (3): 1292. Doi: 10.3390/su17031292.

[7] Mohammadi, F.; and Mirhashemi, M. 2024. An overview of planning for vehicle-to-grid systems with large-scale adoption of electric vehicles. Proceedings of the 2024 Global Energy Conference (GEC). Batman, Turkiye, December. pp. 236–239. New York: IEEE, doi: 10.1109/GEC61857.2024.10881136

[8] Dave, G.; Patel, T.; and Mitra, S. 2025. Global scenario on renewable energy and net zero goal emphasizing Indian standpoint: a short review. Energy Systems: 1-22. Doi: 10.1007/s12667-025-00728-5

[9] Kela, K.B.; Suthar, B.N.; Arya, R.; Singh, P.; and Arya, L.D. 2025. Reliability Performance Optimization and Voltage Sag Mitigation for Radial Distribution Systems with Distributed Generations. GMSARN International Journal 19: 675-686.

[10] Jeon, S., and Bae, S. 2025. Integrated optimization for sizing, placement, and energy management of hybrid energy storage systems in renewable power systems. Journal of Energy Storage 106: 114793. Doi: 10.1016/j.est.2024.114793.

[11] Pham, L.H.; Phan, T.T.; Phan, K.D.T.; and Nguyen, P.H. 2024. Optimizing the efficiency of photovoltaic distributed generation in the distribution system. Journal of Advanced Engineering and Computation 8 (1): 19-28. Doi: 10.55579/jaec.202481.440.

[12] Shah, S.N.H., Waqar, A., Raza, A., Qaisar, S.M., Al-Ammar, E.A., and Junaid, M. 2025. Power factor improvement in regional distribution feeders with optimal allocation of distributed generators and shunt capacitors. Proceedings of the 2025 4th International Conference on Computing and Information Technology (ICCIT). Istanbul, Turkey, April. pp. 672–677. New York: IEEE.

[13] Bolaños, R.I.; Pinto Vega, H.; Grisales-Noreña, L.F.; Montoya, O.D.; and Hernández, J.C. 2025. Intelligent active and reactive power management for wind-based distributed generation in microgrids via advanced metaheuristic optimization. Applied System Innovation 8 (4): 87. Doi: 10.3390/asi8040087.

[14] Rajakumar, P.; Balasubramaniam, P.M.; Munimathan, A.; Alwetaishi, M.; Gulbarga, M.I.; and Senthilpari, C. 2025. Osprey optimization algorithm for distributed generation integration in a radial distribution system for power loss reduction. Scientific Reports 15 (1): 18775. Doi: 10.1038/s41598-025-18775-4.

[15] Rajakumar, P.; Balasubramaniam, P.M.; Parimalasundar, E.; Suresh, K.; and Aravind, P. 2025. Optimized placement and sizing of solar photovoltaic distributed generation using jellyfish search algorithm for enhanced power system performance. Scientific Reports 15 (1): 20755. Doi: 10.1038/s41598-025-20755-4.

[16] Patnaik, S.; Nayak, M.R.; and Viswavandya, M. 2023. Optimal Battery Energy Storage System Management with Wind Turbine Generator in Unbalanced Low Power Distribution System. Advances in Electrical and Electronic Engineering 20 (4): 523-536. Doi: 10.15598/aeee.v20i4.4632.

[17] Fokui, W.S.T.; Ngoo, L.; and Saulo, M. 2022. Optimal integration of electric vehicle charging stations and compensating photovoltaic systems in a distribution network segregated into communities. Journal of Advanced Engineering and Computation 6 (4): 260-275. Doi: 10.55579/jaec.202264.275.

[18] Abeg, A.I.; Islam, M.R.; Hossain, M.A.; Ishraque, M.F.; Islam, M.R.; and Hossain, M.J. 2024. Capacity and operation

optimization of hybrid microgrid for economic zone using a novel meta-heuristic algorithm. Journal of Energy Storage 94: 112314. Doi: 10.1016/j.est.2024.112314.
[19] Duan, F.; Eslami, M.; Khajehzadeh, M.; Alkhayer, A.G.; and Palani, S. 2024. An improved meta-heuristic method for optimal optimization of electric parking lots in distribution network. Scientific Reports 14 (1): 20363. Doi: 10.1038/s41598-024-71408-0.
[20] Smaili, I.H.; Almalawi, D.R.; Shaheen, A.M.; and Mansour, H.S. 2024. Optimizing PV sources and shunt capacitors for energy efficiency improvement in distribution systems using subtraction-average algorithm. Mathematics 12 (5): 625. Doi: 10.3390/math12050625.
[21] Phan, T.M.; Duong, M.P.; Doan, A.T.; Duong, M.Q.; and Nguyen, T.T. 2024. Optimal design and operation of wind turbines in radial distribution power grids for power loss minimization. Applied Sciences 14 (4): 1462, Doi: 10.3390/app14041462.
[22] Rajakumar, P.; Balasubramaniam, P.M.; Parimalasundar, E.; Suresh, K.; and Aravind, P. 2025. Optimized placement and sizing of solar photovoltaic distributed generation using jellyfish search algorithm for enhanced power system performance. Scientific Reports 15 (1): 20755. Doi: 10.1038/s41598-025-08227-4.
[23] Nazih, A.; Abou El-Ela, A.A.; and Ali, E.S. 2025. Maximizing hosting capacity of renewable energy sources in unbalanced distribution networks using multi-objective optimization approach. Electric Power Systems Research 242: 111458. Doi: 10.1016/j.epsr.2025.111458.
[24] Khasanov, M. Y.; Kamel, S. M.; Kurbanov, A. A.; Jalilov, U. N.; Boliev, A. M.; and Suyarov, A. O. 2023. Optimal Planning of Distribution Network with DG Units and ESS Considering Costs. Proceedings of the 2023 IEEE XVI Int. Sci. Tech. Conf. Actual Problems of Electronic Instrument Engineering (APEIE). November. pp. 1790–1796. New York: IEEE. Doi: 10.1109/APEIE59731.2023.10347572.
[25] Kien, L.C.; Van Hien, T.; Ngoc Tram, H.D.; and Pham, T.D. 2025. Optimal integration of renewable energy–based distributed generation units in radial distribution system. International Transactions on Electrical Energy Systems 2025 (1): 8694811. Doi: 10.1155/etep/8694811.
[26] Nguyen, T.T.; Nguyen, T.T.; and Duong, M.Q. 2022. An improved equilibrium optimizer for optimal placement of photovoltaic systems in radial distribution power networks. Neural Computing and Applications: 1-30. Doi: 10.1007/s00521-021-06779-w.
[27] Daravath, R., and Bali, S.K. 2025. Optimal distributed energy resources placement to reduce power losses and voltage deviation in a distribution system. Iranian Journal of Science and Technology, Transactions of Electrical Engineering 49 (2): 725-744. Doi: 10.1007/s40998-024-00780-4.
[28] Chanbasha, S.; Jayakumar, N.; and Kumar, N.B. 2025. DG allocation for radial distribution system through optimal sizing in radial power distribution network using hybrid redfox pathfinder optimization. Multimedia Tools and Applications 84 (16): 16605-16629. Doi: 10.1007/s11042-024-16505-9.
[29] Maurya, P.; Tiwari, P.; and Pratap, A. 2025. Puma optimizer technique for optimal planning of different types of distributed generation units in radial distribution network considering different load models. Electrical Engineering 107 (3): 2777-2828. Doi: 10.1007/s00202-024-01877-6.
[30] Bendriss, B.; Sayah, S.; and Hamouda, A. 2025. A novel improved Frilled Lizard algorithm for solving the optimal planning problem of renewable energy sources within distribution grids under uncertainties. Energy Conversion and Management 326: 119465. Doi:10.1016/j.enconman.2024.119465.
[31] Fokui, W.S.T.; Rene, E.A.; and Mtonga, T. 2024. Integration of photovoltaic and DSTATCOM in the distribution network using Rat Swarm Optimization technique. Journal of Advanced Engineering and Computation 8 (3): 144-157. Doi: 10.55579/jaec.202483.460.
[32] Seyyedabbasi, A., and Kiani, F. 2023. Sand Cat swarm optimization: A nature-inspired algorithm to solve global optimization problems. Engineering with Computers 39 (4): 2627-2651. Doi: 10.1007/s00366-022-01604-x
[33] Bai, J.; Nguyen-Xuan, H.; Atroshchenko, E.; Kosec, G.; Wang, L.; and Wahab, M.A. 2024. Blood-sucking leech optimizer. Advances in Engineering Software 195: 103696. Doi: 10.1016/j.advengsoft.2024.103696.
[34] Global solar atlas. Retrieved from https://globalsolaratlas.info/map?c=13.144019,109.340332.

APPENDIX

Table A1: The solution achieved by the two applied algorithms compared to other ones in Case 1

Variable	SFO [20]	COA [20]	MFA [20]	WSA [20]	IEO [26]	SCSO	BLSO
DSG 1 (node)	12	4	9	9	9	8	66
DSG 2 (node)	32	67	33	33	33	66	8
DSG 3 (node)	72	80	61	62	61	33	33
P_{DSG1} (kW)	354.6	31.2	700	950	1000	1095	525
P_{DSG2} (kW)	1059.2	677.9	500	730	800	525	1095
P_{DSG3} (kW)	568.6	421.9	831.2	440	500	675	675
EAPL (kW)	153.6	152.2	151.79	150.7	149.732	148.662	148.662

Table A2. The solution achieved by the two applied algorithms compared to other ones in Case 2

Variable	ALO [27]	AOA [27]	CSA [27]	FPA [27]	SCSO	BLSO
DSG 1 (node)	67	51	28	9	66	66
DSG 2 (node)	9	11	66	59	33	33
DSG 3 (node)	48	66	52	44	8	8
P_{DSG1} (kW)	831.48	592.83	968.04	899.96	590	610
P_{DSG2} (kW)	1146.58	1070.65	869.85	894.96	770	780
P_{DSG3} (kW)	464.49	779.07	604.67	647.63	1180	1160
Q_{DSG1} (kVar)	0.895	0.850	0.867	0.864	365.6492	378.044
Q_{DSG2} (kVar)	0.856	0.858	0.855	0.851	477.2031	483.4006
Q_{DSG3} (kVar)	0.894	0.858	0.886	0.876	731.2983	718.9034
EAPL (kW)	42.432	39.70	42.537	43.082	28.921	28.897